Thermo-Mechanical Finite Element Analysis and Experimental Validation of Weld Induced AngularDistortion in MMAW Butt Welded Plates.

A.V.Damale[1*], Dr.K.N.Nandurkar[2]
1. College of Engg. Kopargaon, Dist.- Amednagar- (M.S.) India

2. K.K.W. Institute of Engg. Education and Research Nashik, (M.S.) India

*Corresponding Author

Abstract

Welding induced distortion is one of the critical defects in the weld structures. Angular distortion is most pronounced which badly affects the weld structures. Non uniform heating during welding develops this angular distortion. Various methods are available to control/minimize the welding distortions. One of the methods available to control this distortion is to provide angular distortion in the negative direction before the welding if the magnitude of the same is predictable. In the present study three-dimensional transient thermal analyses is done for predicting angular distortion. The transient thermal heat source was used to simulate the weld phenomenon. The element birth and death technique was used for simulating filler material deposition. The thermal model was verified by comparing the temperatures obtained from the thermal analysis with experimental results and verification of structural model was done by comparing the measured and predicted angular distortion. Transient thermal and non-linear structural analyses were carried out in order to predict angular distortions. The FEM analysis and experimental verification is done for MMAW.

Keywords: finite element analysis, Manual Metal arc welding, transient thermal analysis, temperature distribution, element birth and death method, thermomechanical analysis, angular distortions.

1. Introduction

Welding, among all mechanic al joining processes, is being increasingly employed owing to its advantages in design flexibility, cost savings, reduced overall weight and enhanced structural performance. However, welding induces various types of distortions like angular, transverse, longitudinal etc.[11]. Distortions introduce residual deformation that complicates the assembly of welded structures and reduces their quality. Also, in certain applications, this distortion may result in the structure being useless.[11].To assess the effects of welding on structure efficiently, and in turn to implement various distortion mitigation techniques, a validated method to predict welding induced distortion is necessary. Structures made of relatively thick components, welding can introduce significant angular distortion , which causes loss of dimensional control, structural integrity and increased fabrication costs due to poor fit-up between panels.[2] A predictive analysis technique can determine the susceptibility of a particular design to angular distortion . Furthermore, a predictive analysis tool can assist in the selection of geometry and welding conditions that will minimise distortion. Flame straightening is commonly used to correct the buckling distortion resulting from welding processes; which is a labour intensive and costly process. Moreover , it is a corrective action after the damage is done rather than a preventive measure[3], which is generally desirable in engineering processes. The use of the Finite Element Method (FEM) in product development is now well established. Its use in manufacturing processes is increasing and is part of the field of new applications in computational mechanics. The most important reason for this development is the industrial need to improve productivity and quality of products and to have better understanding of the influence of different process parameters [6]. The modeled phenomena play an important role at various stages of the production of steel parts, such as welding, heat treatment and casting, among others. Accordingly, FEM techniques have been used in the prediction of welding residual stress and distortion for more than two decades. Additional complexities are involved in the FEA of welding compared with other thermomechanical processes because of factors such as temperature and history dependent material properties; high gradients of temperature, stress and strain fields with respect to both time and spatial coordinates; large deformations in thin structure s and phase transformation; and creep phenomena[8].

Earlier studies of welding accounted for the non-linearities caused by temperature dependent material properties and plastic deformations. The majority of those analyses were limited to two dimensions (2D) on the plane [7-8] perpendicular to the welding direction ; however, good

correlations have been observed between the numerical predictions and experimental results.

2. Modelling methodology

In the present work three-dimensional finite element analyses were carried out for predicting the transient temperature distributions and angular distortions of multi-pass manual metal arc-welded 'V' butt joints (i.e. joints with 'V' groove preparation) by taking into consideration, (a) moving heat source; (b) temperature-dependent thermal and mechanical material properties; (c) layer-wise application of heat flux for each pass of welding; (d) element activation and deactivation for incorporating filler material deposition in each pass; (e) deactivation of elements of the second weld pass while applying the heat flux and subsequent cooling to the elements of the first pass;(f)incorporating an appropriate material model for simulating elastic–plastic behaviour of the mild steel weld and base metal. Heat flux was applied layer-wise for each pass of welding, while considering filler material deposition and moving heat source to obtain the transient thermal profiles. Half plate was modelled [fig.1 and fig.2] due to the axisymmetric condition and to minimize the memory requirement and analysis time required. The thermal profiles were matched with the experimental data. Angular distortions before and after welding of the plates were also measured.

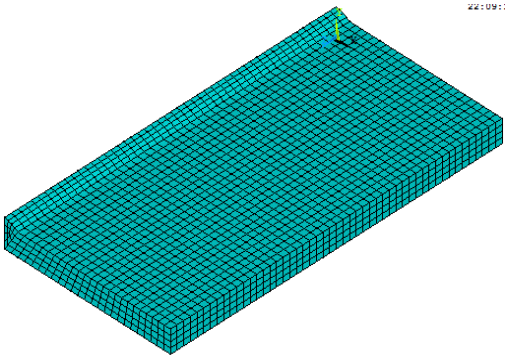

Fig. Half Meshed Model

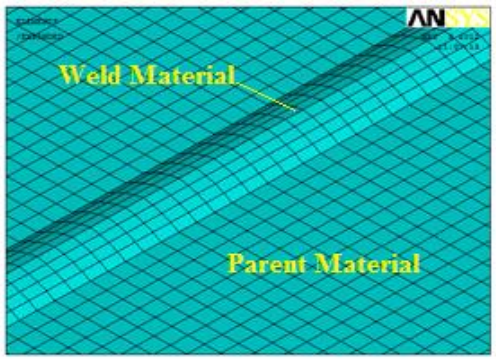

Fig.2 Meshed Filler and parent material (Expanded plate)

Transient thermal and non-linear structural analyses were carried out for predicting angular distortion. The model was further verified by comparing the predicted and experimentally obtained angular distortions. The composition of the mild steel plates used in the experiments is shown inTable 1. The thermomechanical properties of mild steel [11] used for modelling temperature distributions and distortions are shown in Table 2. Solidus ($T_{solidus}$) and liquidus ($T_{liquidus}$) temperatures of the mild steel used in the analysis were considered to be 1435 and 1500^0C.The density of the mild steel used in the analysis was taken as 7850 kg/m^3 [11].

2.1 Thermal Model

The heat source was modelled as a distributed heat flux depending on arc spread. The rate of arc travel and current were varied and these parameters were noted along with the temperature data. The radius of arc spread was estimated by considering the electrode diameter and bead widths of welds formed during experiments. This arc radius was used for transient thermal analysis with a moving arc and the temperature profiles were verified with the experimentally measured ones. After obtaining the temperature profiles for each job the thermomechanical analyses were carried out for predicting the angular distortions.

The moving heat load applied in the finite element model was taken as a distributed heat flux as given by equation one[9]. A schematic diagram of a one-sided but joint is shown in Fig. 6. Meshing and modelling of the one-sided butt joints are shown in fig.1 and fig.2. The moving heat load was applied on the area bounded by the weld lines as shown in Fig. 3(a)-3(b) and except for this area other areas of the plate are subjected to heat loss due to convection. Details of the temperature zones of the weld arc are shown in fig.4. shows In this analysis the convection loss is taken as 15 W/mK [9], and the supplied heat flux is

$$Q_{\sup(r)} = \frac{3Q_e}{\pi \bar{r}^2} e^{\left[-3\left[\frac{r}{\bar{r}}\right]^2\right]} \quad (1)$$

Where $\bar{r}$ is the region in which 95 percent of heat flux is concentrated [9] and $Q_e = \eta VI$. Where η is the arc efficiency, V is the voltage and I is the current.

2.2 Assumptions

The following assumptions were made in the presentfinite element analysis.

1. Density is not affected due to thermal expansion.

Table1Compositionofthe steelusedinthe experiments [11]

C(%)	Si(%)	Mn (%)	P(%)	S(%)	Ni(%)	Cr(%)	Fe(%)
0.15584	0.17774	0.45330	0.17975	0.06918	0.1324	0.01567	98.8413

Table2Thermaland mechanicalpropertiesofmild steel[11]

Temperature (^{0}C)	Thermal Conductivity (W/mK)	Specific Heat (J/kgK)	Enthalpy (J/m^3)	Poison'sratio	Yield Stress (MPa)	Young's Modulus (GPa)	Thermal expansion of Coefficient (10^{-6}/^{O}C)
0	51.9	450	1×10^9	0.2786	290	200	10
100	51.1	499.2	2×10^9	0.3095	260	200	11
300	46.1	565.5	2.65×10^9	0.331	200	200	12
450	41.05	630.5	3.8×10^9	0.338	150	150	13
550	37.5	705.5	4.1×10^9	0.3575	120	110	14
600	35.6	773.3	4.55×10^9	0.3738	110	88	14
720	30.64	1080.4	5×10^9	0.3738	9.8	20	14
800	26	931	5.23×10^9	0.4238	9.8	20	15
1450	29.45	437.93	9×109	0.4738	—	2	—
1510	29.7	400	1.1×10^{10}	0.499	—	0.2	—
1580	29.7	735.25	1.1×10^{10}	0.499	0.0098	0.00002	—
5000	42.2	400	1.25×10^{10}	0.499	0.0098	0.00002	15.5

2.Linear Newtonian convective cooling was assumed. No forced convection was considered.
3.Convective cooling was assumed on all surfaces except the weld zone.

4. The heat source was assumed to have a Gaussian distribution of heat flux.

5. Arc efficiency (n = 0.75) [10] was taken to account for other losses.

The governing differential equation for heat conduction in a solid without heat generation is given by

$$\frac{\partial}{\partial x}\left[K\frac{\partial T}{\partial x}\right]+\frac{\partial}{\partial y}\left[K\frac{\partial T}{\partial y}\right]+\frac{\partial}{\partial z}\left[K\frac{\partial T}{\partial z}\right]=\rho c\frac{\partial T}{\partial t}.2)$$

Where, K is the thermal conductivity, T is the temperature,ρ is the density of material, c is the specific heat and t is the time.

4.2.1 Boundary conditions

(a) ***First boundary condition.***A specified initial temperature for the welding that covers all the elements of the specimen:

$T = T_\infty$ for $t = 0$ (3)

(b)***Second boundary condition***. The arc heat acting over surface S_1 is given by

$q_n = - q_{sup}$

or$-K\frac{\partial T}{\partial n} = - q_{sup}$ on the surface S_1 for t >1 (4)

The quantity $q_n$represent the component of the conduction heat flux vector normal to the work surface. The quantity q_{sup} represents the heat flux supplied to the work surface in w/m^2, from an external welding arc.

(c)***Third boundary condition:*** The heat loss due to convection (q_{conv})over surface S_2 is given by

$-K\frac{\partial T}{\partial n} = - h_f(T_\infty - T)$ on surface s_2 for t > 0. (5)

To avoid the sharp change in the value of specific heat, the enthalpy was used as the material property. This was done by defining the enthalpy of material as a function of temperature [9].

2.3 Structural model

The stress–strain relationship can be represented as

$\{\sigma\} = [D]\{\varepsilon^e\}$ (6)

Where,

$\{\sigma\}$ = stress vector = $[\sigma_x\ \sigma_y\sigma_z\sigma_{xy}\sigma_{yz}\sigma_{zx}]^T$

[D] =stress-strain matrix

$\{\varepsilon^e\} = \{\varepsilon\} - \{\varepsilon^t\}$(7)

$$\{\varepsilon^t\} = \Delta T\ [\alpha_x \alpha_y \alpha_z\ 0\ 0\ 0]^T \qquad (8)$$

Where $\Delta T = T_n - T_\infty$ and T_n is the instant temperature at the point of interest.

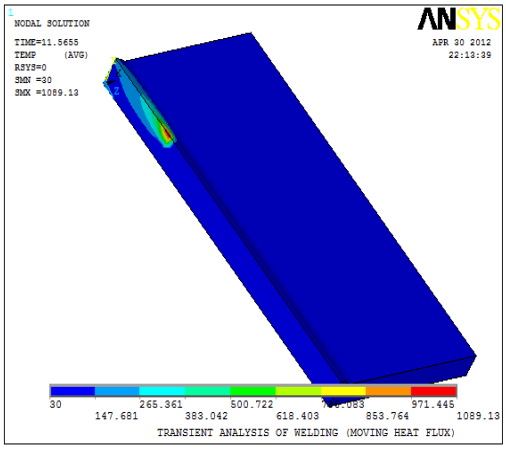

(a) At t= 11.56 sec

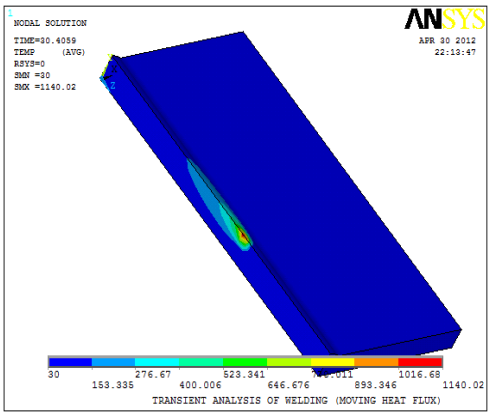

(b) t= 20.40 sec

Fig.3 Transient heat source

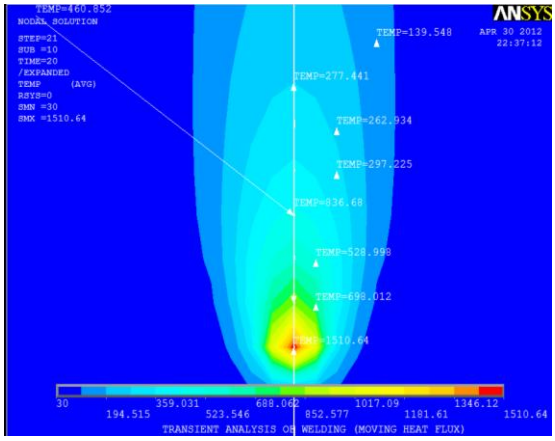

Fig.4 Temperature zones of the transient heat source of FE model

Considering the plastic strains, equation (7) can be written as

$$\{\varepsilon^e\} = \{\varepsilon\} - \{\varepsilon^t\} - \{\varepsilon^p\}.$$

Transient thermal and non-linear structural analysis was done for predicting angular distortion. For each pass of welding the temperature history from the thermal analysis in every load step was used as the thermal loading in the structural analysis. The structural analysis involves large displacements (strain) and a rate-independent thermo-elasto-plastic material model with temperature-dependent material properties incorporated into the modelling. Kinematic work hardening together with the von Mises yield criterion and associative flow rules [10] were assumed in the analysis. In the structural analysis boundary conditions that prevented rigid body motions were imposed into the modelling. In the present work eight-noded brick elements were used for the thermal analysis and similar eight-noded elements were used in the structural analysis. The eight-noded brick elements were chosen for required good compatibility in thermomechanical analysis [12]. The solution was obtained using the ANSYS package [12].A user defined subroutine was developed in APDL (ANSYS Parametric Design Language) for the analysis.

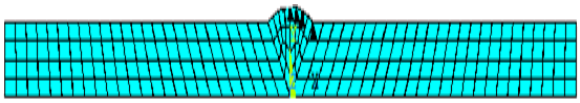

(a)Undistorted plate before welding

(b) Distorted plate after first pass

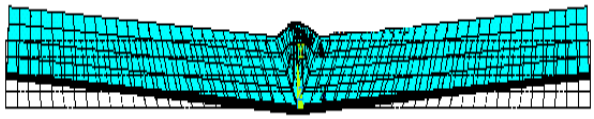

(c) Distorted plate after second pass

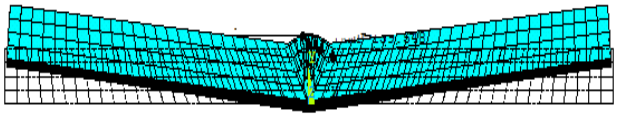

(d) Fully distorted plate after third pass

Fig.5 Specimen at different time conditions

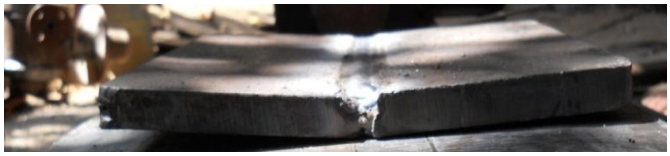

Fig.6 Distorted weld specimen after welding

3. Experimental details

Manual metal arc welding (MMAW) on test samples was carried out with various combinations of welding speed and current whereas the voltage was kept constant. As MMAW can be formed in AC and DC mode, in this experiment DC mode was used with electrode connected to the positive terminal and workpiece to the negative terminal i.e. DCEP mode. Mechanised speed controlling unit (small trolley) was used to keep the constant speed during the welding. During welding, the operators hand was placed on this mechanised unit and the weld speed was controlled by keeping the constant speed of the unit. The Chromel–alumel (K-type) thermocouples were used on the top sides of the plates away from the weld line to record temperature history during welding. The temperature history of the process was noted for each 5 second of time interval.

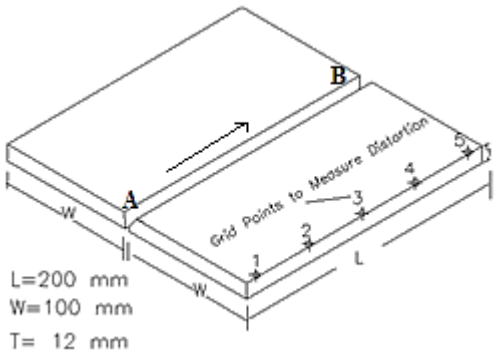

Fig.7 Schematic diagram of specimen with control points for distortion measurements

A typical welding weld specimen size is shown in Fig.7.All plates were welded as a one-sided butt weld in three passes. The length, width and thickness of the plates were 200,100 and 12 mm respectively. The required "V" grooves of the plates were prepared on the vertical milling machine. The length and width of the plates were considered appropriate for finite element modelling purposes taking into account the moving distributed heat source [6].Before starting the welding; the plates were tack welded at 10mm from both the ends to avoid the in-plane rotation of the plates. A skilled welder was used to perform the welding operation. The type filler rods used were of type IS: 814-91: ER 4212X with 450 mm length, 2.15 and 4 mm diameters. The passes were started at point A and finished at point B (Fig.7).A time gap of 1.5 min was given between the successive passes. This duration was utilised to remove the slag formed during the each pass. Care was taken to ensure that the thermocouple connections were not disturbed during this slag removal. Voltage and current were measured during welding on the digital meters mounted on the welding machine. The duration of welding was noted down for each pass. Knowing the weld length, the speed was calculated. The welding and other parameters of the five test pieces are given in Table 3.To measure the angular distortion, the grid points were marked on the workpiece (Fig.7). Mechanical dial gauge mounted on the magnetic stand was used to measure the vertical displacement of the plates.

Table 3.Welding specifications

Job. No.	Current (Amp)	Voltage (Volt)	Welding Speed(mm/s)
1	150	75	3.12
2	160	75	3.68
3	170	75	3.95
4	180	75	4.10
5	185	75	4.23

4. Approaches for FE model validation

To validate the developed FE model, in this paper two approaches are followed. These approaches are thermal model validation and structural model validation. For thermal model validation the thermal profile of the FE model and the actual welding was compared. This was done by measuring the temperature history of the process and observing the FE temperatures in the model at the corresponding points. Predicted and measured angular displacements were compared to validate the structural model. Five butt welded specimens were prepared with different set of process parameters as shown in table 3.

5. Results and discussions

Modeling and meshing of a 12 mm thick multipass-butt joint is shown in fig 1 and fig.2. The meshed size for the filler material and parent material was kept similar and mapped meshing was performed. Predicted and measured temperatures of the first pass for specimen one were noted and are shown infig.8.TC_1 to TC_4 indicates the thermocouples 1 to 4.Both experimental and FE results are plotted in the graphical form in fig.8 For predicted and measured The figure shows that peak temperature rise to about 950^0K.The peak temperature attained goes down with increase in the distance from the weld line. From fig.8 is can be observed that the predicted and measured temperatures are in close agreements with each others. The deformed shape of the plate after each pass of the weld has been shown in fig.5. Fig.5 (a) shows the flat plate before the application of the heat flux. Fig 5. (b), (c) and (d) shows the plates after first, second and third weld pass. From these figures it can be observed that the distortion of the plates has increased with the increase in weld passes from one

to three.Similar trends also observed in the experimental analysis too. However fig. 6 shows distorted plate after final pass of experimental analysis. Close observation of these fig.5 and fig.6 shows that the predicted and measured distortions which are similar in nature.

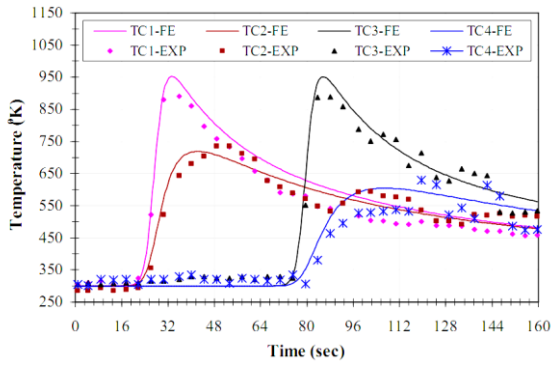

Fig.8 Predicted and measured transient temperatures

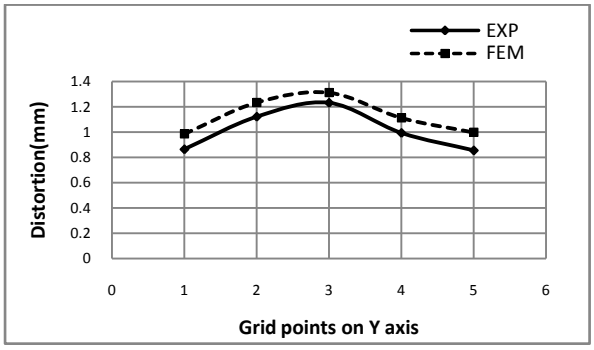

(a) Specimen 1.

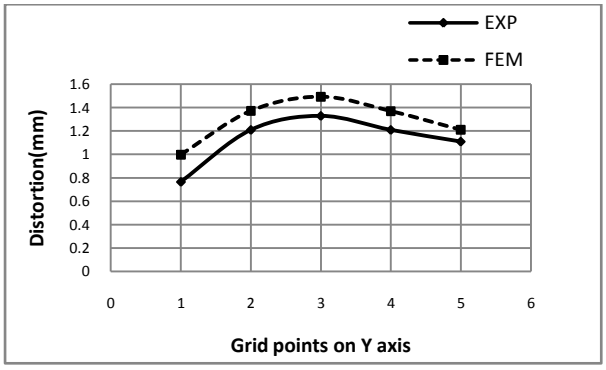

(b) Specimen 2.

Fig.9 (a) to (e) shows the nature on the predicted and measured angular distortions for five specimens. A close observation of theses curves indicates that the predicted and measured distortions are close in agreement to each other. The curves shows the higher values of distortion are found at the mid of the length of workpiece which may be due the stabilization of the weld arc. From fig.9,it can be observed that,FEM results of the angular distortion and the experimental results are in close agreement with each other.

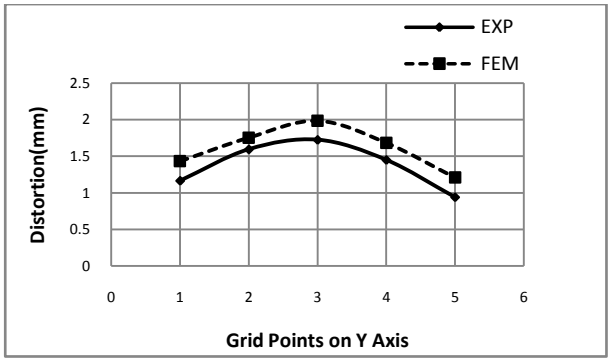

(c) Specimen 2.

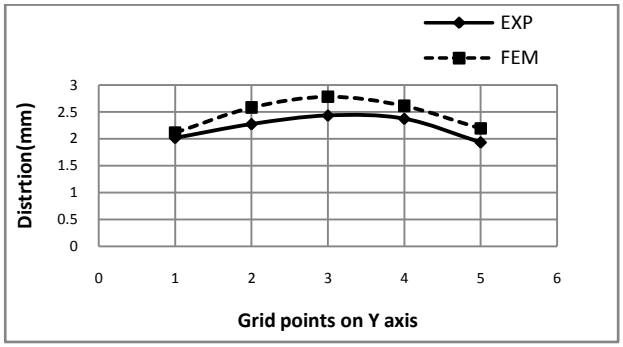

(d) Specimen 4.

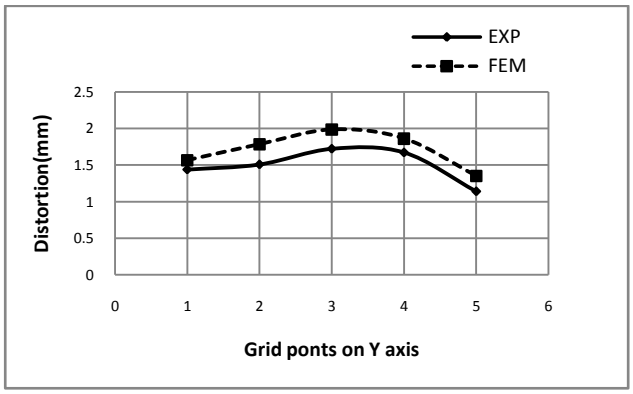

(e) Specimen 5.

Fig.9 (a)-(e) Predicted and measured distortion for tested specimens

6. Conclusions

The following can be stated from the present experimental and modelling investigations on Multi pass manual metal arc welded butt welding.

1. A 3-D finite element model for predicting the temperature distributions and the angular distortions of multipass manual metal arc welded “V” but joints has been developed.
2. Experimental temperature distributions of the “V” butt joints away from the weld line closely matched the values obtained from the finite element modelling.

3. Layer-wise application of heat flux, incorporation of the joint geometry into the modelling and consideration of filler material deposition in the analysis led to temperature distribution profiles that closely matched the experimental values
4. Close matching between modeled and measured angular distortions has been observed.
5. Predicted angular distortion can be used for pre-setting the specimen to control the angular distortion.

References

1. Michaleris P and DeBiccari A., Prediction of welding distortion, Welding journal 1997,76(4),172-180
2. D. A. Price, S. W. Williams, A. Wescott, C. J. C. Harrison, A. Rezai, A. Steuwer, M. Peel, P. Staron and M. Kocak, Distortion control in welding by mechanical tensioning, Science and Technology of Welding and Joining, 2007, 12(7), 620-633.
3. Liam Gannon and K-H Chang, "Effect of welding sequence on residual stress and distortion in flat-bar stiffened plates" Marine Structures ,23 (2010) 385–404
4. D. Camilleri, P. Mollicone andT. G. F. Gray, Computational methods and experimental validation of welding distortion models. Proc. IMechE L: J. Materials: Design and Applications, 2007, 221, 235-249.
5. E.Friedman, ThermomechanicalAnalysisoftheWelding ProcessUsingtheFiniteElementMethod-JournalofPressureVesselTechnology, 1975,97(3),p.206-213,
6. Lindgren.L.E.andKarlsson,L.,DeformationandStressesinWeldingofShellStructures,Int. J.NumericalMethodsinEngineering, 1998,vol.25,pp.635–655,
7. Dong-yang Yan, Ai-ping Wua,, Juergen Silvanus and Qingyu Shi, Predicting residual distortion of aluminium alloy stiffened sheet after friction stir welding by numerical simulation, Materials and Design, 2010, 32(2011), 2284-2291.
8. W. Perret, C. Schwenk, M. Rethmeier, Comparison of analytical and numerical welding temperature field calculation, Computational Materials Science, 2009, 47(2010), 1005-1015
9. Radaj,R.,HeatEffectsofWelding, 1992.,Springer-Verlag, UK
10. ASMMetalsHandbookVolume2-PropertiesandSelectionNonferrousAlloysandSpecial PurposeMaterials,ASMInternational,ISBN0-87170-378-5(v.2).
11. ANSYS 14user'sdocumentation,SAS IPInc,Canonburg, 2005,PA15317,USA,.
12. WeldingHandbookVolume2-Part1:WeldingProcesses,AmericanWeldingSociety2004, ISBN: 0871717298.
13. Pathak A.K., Three-dimensional finite element analysis of heat transfer in arc welding, Phd thesis, 2002, I.I.T. Kharagpur, India.
14. N. R. Mandal, Welding and Distortion, Narosa Publishing House, 2004, New Delhi.